JAAS

Accepted Manuscript

ROYAL SOCIETY OF CHEMISTRY

www.rsc.org/jaas

Instrumental Isotope Fractionation in Multiple-Collector ICP-MS

Francis Albarède[1], Emmanuelle Albalat[1], Philippe Télouk[1]

June 15, 2015

[1]*Ecole Normale Supérieure de Lyon and CNRS, 69007 Lyon, France*

Corresponding author: albarede@ens-lyon.fr

Revision #1

Abstract

This work addresses the issue of how isotope mass biases in modern Multiple-Collector Inductively Coupled Plasma Mass Spectrometers (MC-ICP-MS) changes with increasing efficiency of ion transfer through the instrument, which is known as transmission (τ). For any element, when all the ions introduced into the source are accounted for at the collector, the instrumental mass bias must vanish With the latest cone designs, such as Thermo Finnigan jet cones, transmissions in excess of 2 percent are now obtained for heavy elements and coincide with smaller values of instrumental isotope fractionation factors. Transmission of ions across the entire mass range has been measured on a Thermo Neptune Plus equipped with standard and jet cones. It was found that transmission τ of elements above mass 40 increases linearly with the atomic weight. Comparing this relationship with the well-established linear dependence of ion energy with atomic mass indicates that high transmission is intimately related to the thermodynamic reversibility of the gas flow in the interface. Instrumental isotope fractionation obeys an exponential law with β as a coefficient. Instrumental isotopic fractionation is due to the transverse spread of the beam inherited from Ar thermal movements at the high temperatures of the plasma. It was found that, for $\tau > 0.002$, the exponential law coefficient $\beta \approx -0.24 \pm 0.02 \ln \tau$ in contrast to $\beta \approx 2$ at lower transmission. The exponential mass fractionation coefficient can be approximated by the following law: $\beta{=}\beta_0(1-\tau^\gamma)$

1 Introduction

Multiple-Collector Inductively Coupled Plasma Mass Spectrometers (MC-ICP-MS) have become the instrument of choice to measure the isotope compositions of soluble elements. MC-ICP-MS advantages over Thermal Ionization Mass Spectrometers (TIMS) are multiple: (1) essentially any element can be ionized by electron ionization and exchange with Ar^+, (2) the isotopic mass bias of the instrument for a particular element can be estimated by normalizing its isotope abundances to the bias measured on an element of nearby atomic masses, for example Cu and Zn or Pb and Tl, and (3) the isotopic mass-dependent bias of the instrument can be corrected by bracketing the sample run with standard runs, and (4) the isotope composition of nearly all elements with as few as two isotopes (with exceptions such as H, C, O, N, Ar can be measured. MC-ICP-MS main drawbacks are the prevalence of isobaric interferences, which high-resolution capabilities are bringing to resolution at least for heavy elements, and a so-far smaller ion transmissions relative to TIMS, which new interface technologies and in particular cone geometry are also in the process of resolving. To date, transmission of two ions collected for 100 atoms of heavy elements such as Pb and U introduced into the plasma is the new standard achieved by modern commercial MC-ICP-MS instruments. The major concern of MC-ICP-MS techniques is the rather strong mass bias affecting isotope measurements (in the percent range) relative to the permil range offered by TIMS. Achieving < 1 ppm precisions as with TIMS remains the major challenge of MC-ICP-MS.

Instrumental mass-fractionation on MC-ICP-MS instruments (mass bias) can now be made stable and reproducible by the analyst, even if the underlying physics is not perfectly understood. In the early days, a range of mass fractionation laws has been used to correct the mass bias, typically laws qualified as linear, exponential, power, kinetic, etc [1,2]. Albarede et al. [3] demonstrated that all these laws only reflect particular ways of expanding machine transmission as a function of mass difference using different functional relationships. Maréchal et al. [4] provided a unified conceptual framework in the form of a *Generalized Fractionation Law* (GFL), which covers most of the instrumental fractionation laws with the exception of the linear law, which is not internally consistent. Two decades of intensive work have demonstrated that the exponential mass fractionation law

$$\frac{n^j/n^i}{n_0^j/n_0^i} = \frac{n^j/n_0^j}{n^i/n_0^i} = \frac{\tau_j}{\tau_i} = \left(\frac{M_j}{M_i}\right)^{\beta} \tag{1}$$

where n stands for the number of ions, i and j for two isotopes of the same element, M for the atomic mass, β for the fractionation factor, and τ for the transmission of the mass spectrometer for a particular nuclide is suitable for most analytical data. Unsubscripted n's are measured values, while the 0 subscript signals abundances in the original solution. The exponential law accounts for most of the measured mass bias, but the physics of mass fractionation remains too elusive for the issue to be settled. It was found by many groups that a value of β of $\sim$2 fits most of the elements across the mass range, a remarkable feature for which Maréchal et al. [4] discussed possible interpretations. This value reflects that light isotopes are preferentially lost from the beam, which has received a variety of interpretations, notably the effect of space charge.

Increased mass spectrometer transmission both raises new perspectives and demands a return to the physics of mass bias. It is clear that when efficiency of ion transfer through the instrument is total, i.e., when transmission increases to 100 percent for each of the isotopes of a given element, mass fractionation should vanish and β should be zero. This argument is, of course, not relevant to mass-dependent fractionation during natural processes or sample preparation. Mass spectrometers with full-transmission may not be available anytime soon, but transmission is being continuously improved. With new cone designs, such as Thermo Finnigan Jet sampler cones combined with X-skimmer cones, yields approaching 2 percent are now observed to coincide with smaller values of β, typically 1.3 or less, in contrast with the β=2 of the first instruments constructed 20 years ago. A reduction of the mass bias by about half has been first noted for tungsten [5].

The purpose of the present work is to investigate how the increase of transmission by a new generation of cones, known as Jet cones, affects the transmission of a Thermo Finnigan MC-ICP-MS Neptune Plus. We compared transmission by Jet cones and standard cones from Li to U. We also compared the transmission law derived from elements with the law derived from the different isotopes of the same element. We first summarize the principles underlying the physics of isotopic bias in ICP-MS. We will describe the experimental conditions used for the runs, then present the results and discuss their interpretation in terms of processes and propose a predictive law relating mass fractionation and transmission.

Instrumental mass-independent effects, such as odd-even and nuclear volume effects, will not be covered in this work. Although their existence has been unambiguously identified and their origin discussed [5,6], their amplitude is small and the combination of internal (or external) isotope normalization with sample-standard bracketing [3] minimizes the incidence of these processes for sample analysis

2 Background

This part will briefly review some aspects of charged beam focusing relevant to MC-ICP-MS. As emphasized by Niu and Houk [7], neutral argon is the quasi-exclusive species in the plasma of an ICP torch. Ions should therefore collide with neutral argon far more frequently than with themselves or with any other species as they pass through the cones. Likewise, the most abundant ion species is Ar^+ and the ion beam focusing properties are defined by those of the Ar^+ beam properties.

The total kinetic energy of a gas E^{tot} with atomic mass m is the sum of the internal energy (thermal agitation) E^{int} and of hydrodynamic energy (energy of the center of mass) E^{hydr}. Summing over N molecules, each with their velocity v_i, this principle reads

$$E^{\text{tot}} = m\sum_i v_i^2 = m\sum_i \left(v_i - \overline{v}\right)^2 + mN\overline{v}^2 = E^{\text{int}} + E^{\text{hydr}} \tag{2}$$

In this equation, $\overline{v}$ is the velocity of the center of mass. In the torch at near-atmospheric pressure, the mean free path is very short (typically < µm). Hence collisions are very frequent and the distribution of $v_i - \overline{v}$ follows a Maxwell velocity distribution

$$f(v) = 4\pi\left(v - \overline{v}\right)^2 \left(\frac{m}{2\pi kT}\right)^{3/2} \mathrm{e}^{-\dfrac{m\left(v-\overline{v}\right)^2}{2kT}} \tag{3}$$

with a standard deviation σ= $\sim \sqrt{kT/m}$, where T is the temperature and k the Boltzmann constant. At the high temperatures of the plasma (>6000 K or $\sim$ 0.5 eV), most of the energy is thermal and E^{hydr} can be neglected. Upon extraction of the gas into the sampler cone, expansion in vacuum produces a shock barrel and a Mach disk [8]. In a free-drift space (no external electrostatic field), the total kinetic energy of the gas is conserved and most of the internal energy E^{int} is adiabatically converted into largely unidirectional hydrodynamic energy E^{hydr}. The internal energy of monatomic Ar being $\frac{3}{2}kT$, the maximum mean-square velocity after the cones is

$$v_{\max} = \sqrt{\frac{3kT}{m}} \tag{4}$$

For Ar at a temperature of 6000 K, the maximum gas hydrodynamic velocity along the mass-spectrometer axis is $\sim$1930 m s^{-1}. Temperature after expansion was estimated at $\sim$ 150 K, as in conventional ICP-MS sources of the mid to late 90s [7], while modern interfaces equipped with high-speed pumps removes residual gas and ‘cool’ the beam quite efficiently. This transverse velocity dispersion is about one percent of the velocity of Ar$^+$ at the entrance slit of the mass spectrometer acquired in the accelerating field defined by the voltage V

$$v_{\mathrm{Ar}^+} = \sqrt{\frac{2eV}{m_{\mathrm{Ar}}}} \tag{5}$$

In contrast with the thermal velocity distribution, which is controlled by momentum exchange among gas atoms, molecules, and ions, the hydrodynamic velocity of Ar^+ and other ions is imposed by the velocity of the expanding Ar neutrals. Like in a turbine, the maximum gain in hydrodynamic kinetic energy is equal to the variation of enthalpy H of the expanding gas. The initial enthalpy of Ar neutrals is

$$H_{\mathrm{Ar}}^{\mathrm{int}} = \frac{5}{2}kT \tag{6}$$

For ions i at neutral Ar velocity, we obtain the very important relationship:

$$\frac{1}{2}m_i v_i^2 = \frac{m_i}{m_{\mathrm{Ar}}}\Delta H_{\mathrm{Ar}}^{\mathrm{int}} = \frac{m_i}{m_{\mathrm{Ar}}}\left(\frac{5}{2}k\Delta T\right) \tag{7}$$

where ΔT is the longitudinal temperature drop in the cone. This relationship has been used to explain the linear correlation between ion kinetic energy and their atomic mass [5,9-10].

The mean free path in the gas changes from about 1 µm in the plasma to >1 m in the vacuum of the instrument [7], so that gas regime changes from a thermalized state to collisionless 'laminar' flow. One of the causes of the mass bias is therefore the persistence of a transverse component of thermal velocity in the Ar^+ beam inherited from the Ar velocity distribution in the torch. Because of the longitudinal cooling by acceleration, a charged particle beam is not in a 3D equilibrium: the longitudinal and transverse temperatures are quite different and there is little cooling of the transverse component.

The standard deviation of transverse velocity is $\sqrt{kT/m}$, while the transit time between the source and a transverse plane at the distance L between sampler aperture and the extraction-lens crossover is $\sqrt{2m/eV} \times L$, so that the thermal spread of the beam size is

$$\sigma = \sqrt{2kT/eV}\,L \tag{8}$$

If $\sigma > a\mathcal{M}$, where a is the radius of the skimmer orifice and $\mathcal{M}$ optical magnification at L, the current density $J\left(r\right)$ at the distance r of the optical axis is [11]

$$J\left(r\right)=\frac{J_0}{\mathcal{M}^2}e^{-\dfrac{r^2}{2\sigma^2}}\left(1-e^{-\dfrac{\mathcal{M}^2a^2}{2\sigma^2}}\right) \tag{9}$$

in which J_0 is the density in the absence of thermal spreading.lthough thermal broadening at a given temperature has therefore no effect on the *average* beam size [12], the transverse velocity distribution down the beam axis [12-15] shows a near-gaussian distribution of the current density across the beam and the mass-dependent [4,16], high-radial velocity tail of the distribution is expected to be lost and produce an isotopic bias. A transverse gaussian distribution of charge density was indeed assumed by Maréchal et al. [4] in their discussion of the instrumental mass bias.

An additional effect that has been called on to account for mass fractionation in ICP-MS is the beam broadening by the mutual Coulombian repulsion of charges [7, 15, 17-19]. It is known as ‘space charge’ or self-field effect. Multiple authors suggested that space charge is a major cause of mass bias for MC-ICP-MS [20-22], while others challenged that view [23]. The maximum Ar^+ beam intensity $J_{\max}$ between the skimmer and the entrance slit is given by the Child-Langmuir equation [9,10], which can be written as

$$J_{\max}=\frac{4}{9}\epsilon_0\left(\frac{2e}{m}\right)^{1/2}\frac{V^{3/2}}{L^2}=\frac{4}{9}\epsilon_0 v_{\mathrm{Ar}^+}\frac{V}{L^2} \tag{10}$$

where ϵ_0 is vacuum permittivity, V the ion energy, and L the distance travelled by the ions across the acceleration stage. As pointed out by Niu and Houk [3], space-charge effect, which only applies to the major ions Ar^+, is significant for quadrupole ICP-MS in which ions are not accelerated (drift field). In magnetic-sector, and therefore in MC-ICP-MS, where ions are accelerated to 4-10,000 V, the effect should only be noticeable right behind the skimmer where ion energy is still small. With Gillson et al.’s [12] simplifying assumptions for cone geometry, and a typical acceleration of 6000 V, $J_{\max}$ should be ∼0.6 A, i.e., six orders of magnitude larger than the 0.45 μA of the measured ^{40}Ar^{+} beam, so that space charge should be very small. Other ions with m >40 should spread even less than ^{40}Ar^{+} and remain confined inside the Ar beam: by virtue of the Gauss theorem, this confinement should reduce space charge effects even further. For the same reason, the effect of space charge is quite noticeable when heavy ions are added to lighter analytes, e.g., U to Co [12] and Pb [24]: space charge effect due to traces of heavy ions is a significant component of the broader 'matrix effect'.

3 Analytical techniques

The analytical conditions used for the Neptune Plus are described in Table 1. All the data have been obtained under 'dry plasma' conditions with the help of an Aridus 2. The values of transmission are those of optimum transmission, which allows a stable isotope composition to be reproduced with a 2-σ precision of 0.05 permil. Uncertaintes on transmission values are <20 percent. For elements that are routinely measured for isotope compositions (Li, Mg, Cu, Zn, Sr, Zr, rare-earth elements, Hf, Tl, Pb, U), we found that 2σ uncertainties on the fractionation factor β are < 0.05. β values shifting outside this range indicate that cones have to be replaced. The calculated β values depend to some extent on the assumption that at least one isotope ratio is absolutely known in the reference solution. For example, a one permil change of the ^{205}Tl/^{203}Tl and ^{65}Cu/^{63}Cu reference values shifts β by 0.10 and 0.03, respectively. The standard solutions and the reference isotope ratios used to calculate the β values are given in Table 2. Concentrations were varied in order to explore a range of voltage for the leading peak extending from 5 to 45 volts. Standard solutions used with the jet cones were diluted by a factor of 10 with respect to those used with the standard cones

Before we compare the variations of transmission among different elements (Li, Na, Mg, Al, Ca, Cu Zn, Zr, Nd, Sm, Hf, Tl, Pb, and U), we will

Table 1: *Neptune Plus parameters.*

Mass spectrometer settings	
RF power	1200 W
Cool gas	15 l/min
Auxiliary gas	∼0.9 l/min
Sample gas	∼1.1 l/min
Aridus desolvator settings	
Spray chamber temperature	110°C
Desolvating membrane temp.	160°C
Ar flow	∼9 l/min
N_2 flow	∼0.06 l/min
Nebulizer	Savillex 100 µl/min
Jet cones	Jet sampler + X skimmer
Standard cones	Std sampler + H skimmer
Measurements settings	
Mass resolution	Low (∼400)
Acquisition	40 cycles
Integration time	4 s
Uptake time	90 s
Ar^+ beam	0.45 µA

examine those inferred from the isotopic abundances of a particular element. The isotopic bias must be recast into a transmission range and this can be done in the following way. The total transmission τ of a particular element can be recast as a function of the transmission τ_i of each isotope i and of the isotopic abundance x_i^0 of i in the element:

$$\tau = \frac{\sum n_i}{\Sigma n_i^0} = \sum \frac{n_i}{n_i^0} \frac{n_i^0}{\sum n_i^0} = \sum x_i^0 \tau_i \qquad (11)$$

which simply shows that the transmission for an element is simply the sum of the transmission for each isotope weighed by the abundance of the isotope. We then select a reference or ‘normalization’ isotope labelled ‘ref’ and express the elemental transmission as a function of the transmission of the

Table 2: *Standard solutions and reference ratios used to calculate the exponential fractionation factors β.*

Elements	Standard solutions	Reference ratios		Reference
Li	Neptune Tune Solution*	7Li/6Li	12.0392	Chan et al. [31]
Mg	DSM-3	^{25}Mg/^{24}Mg	0.12663	Catanzaro et al. [32]
Cu	NIST SRM 976	^{65}Cu/^{63}Cu	0.4476	Marechal et al. [2]
Zn	JMC 3-0749 L	^{66}Zn/^{64}Zn	0.56502	Marechal et al. [2]
Sr	NIST SRM 987	^{87}Sr/^{86}Sr	0.7103	Raczek et al. [33]
Zr	Alpha Aesar el. solution	^{94}Zr/^{90}Zr	0.3379	Nomura et al. [34]
Sn	Alpha Aesar el. solution	^{117}Sn/^{118}Sn	0.3178	McNaughton & Rosman [35]
Nd	Neptune Tune Solution*	^{143}Nd/^{144}/Nd	0.51196	Wasserburg et al. [36]
Dy	Alpha Aesar el. solution	^{161}Dy/^{163}/Dy	0.75872	Chang et al. [37]
Hf	JMC 475	^{178}Hf/^{177}Hf	1.467168	Blichert-Toft et al. [19]
Tl	Neptune Tune Solution*	^{205}Tl/^{203}Tl	2.38714	Dunstan et al. [38]
Pb	NIST SRM 981	^{207}Pb/^{204}Pb	15.4976	Eisele et al. [39]
U	IRMM 184	^{235}U/^{238}U	0.007257	Hiess et al. [40]

*The Neptune Tune Solution (PN 1149340) is a dilute HNO_3 solution containing Li, Fe, Nd, Hf and Tl (all from Merck KGaA, Germany), Sr(SRM 987), Pb (SRM 981) and U (SRM 3164). SRM: NIST reference standard material. Standard solutions used with the jet cones were diluted by a factor 10 with respect to those used with the standard cones.

reference isotope and make use of the exponential law.

$$\tau = \tau_{\mathrm{ref}} \sum x_i^0 \frac{\tau_i}{\tau_{\mathrm{ref}}} = \tau_{\mathrm{ref}} \sum x_i^0 \left(\frac{M_i}{M_{\mathrm{ref}}}\right)^{\beta} \tag{12}$$

225 and therefore:

$$\tau_{\mathrm{ref}} = \frac{\tau}{\sum x_i^0 \left(\frac{M_i}{M_{\mathrm{ref}}}\right)^{\beta}} \tag{13}$$

Using the exponential law one more time, we can now derive the transmission for an isotope from the elemental transmission of the same element as:

$$\tau_i = \tau_{\mathrm{ref}} \left(\frac{M_i}{M_{\mathrm{ref}}}\right)^{\beta} = \frac{\left(\frac{M_i}{M_{\mathrm{ref}}}\right)^{\beta}}{\sum x_i^0 \left(\frac{M_i}{M_{\mathrm{ref}}}\right)^{\beta}} \tau \tag{14}$$

and finally

$$\tau_i = \frac{M_i^\beta}{\sum x_i^0 M_i^\beta}\tau \tag{15}$$

This equation shows that, in general, transmission should differ only slightly from one isotope to the next. Changing the isotopic abundances x_i^0 from 5 and 95 percent changes the τ_i/τ ratio by 25 percent per a.m.u. at $M_i = 6$ and by 2 percent at $M_i = 200$. As a first approximation, it therefore seems safe to neglect the isotope effect on transmission.

4 Results and Discussion

Table 3 gives the results for a number of ions spanning nearly the entire mass range. Fig. 1 shows that for most of the mass range, transmission τ is proportional to the mass of the analyte with a break at $M_i \approx 40$. The two different scales used in the figure emphasize that the arrays obtained for the standard and jet cones have very similar shapes. Thallium, which has better transmission but higher instrumental mass bias than U regardless of the cone set used, stands out as an exception. It is unlikely to simply reflect an incorrect reference ^{205}Tl/^{203}Tl value for the standard solution

The first remarkable observation is the linear dependence of transmission τ on the mass of the analyte. This observation is reminiscent of the linear dependence of ion kinetic energy on atomic mass [7,9-10]. The consequential correlation between transmission and ion energy is particularly meaningful. It suggests that transmission increases with the enthalpy drop upon expansion within the interface, which, as for gas expanding within a turbine, is maximized when conditions approach reversibility. Increasing the mean free path by using large pumps and reducing friction along the sampler walls by machining their shape should help generate a fully laminar flow and increase expansion velocity.

Table 3: *Elemental transmission* τ *(number of ions at collector per atom in solution) measured at a mass resolution of 400. Transmission is not given for Fe, which demands a much higher resolution to separate the ArO and ArN isobaric interferences.* β *is the measured exponential mass fractionation factor calculated with respect to the reference isotopic ratios of Table 2. Note the remarkably constant value of* $-\beta/\ln\tau$ *measured with jet cones except for Sn.*

	atomic weight	τ % (std)	τ % (jet)	β^* (std)	β^* (jet)	$-\beta/\ln\tau$ (std)	$-\beta/\ln\tau$ (jet)
Li	6.9	0.003	0.03	1.96	1.87	0.19	0.23
Na	23	0.008	0.094				
Mg	24.3	0.016	0.1	1.52	1.47	0.17	0.21
Al	27	0.007	0.111				
Ca	40	0.02	0.153				
Mn	55	0.027	0.225				
Cu	63.5	0.029	0.132	1.38	1.04	0.17	0.17
Zn	65.4	0.037	0.36	1.57	1.46	0.20	0.23
Sr	87.6	0.064	0.5	1.58	1.49	0.21	0.25
Zr	90	0.05	0.415	1.82	1.48	0.24	0.25
Sn	118.7	0.14	0.85		1.69		0.35
Nd	144.2	0.14	0.91	1.75	1.37	0.27	0.28
Dy	162.5	0.18	1.13	1.53	1.0	0.24	0.23
Hf	178.5	0.18	1.23	1.7	1.13	0.27	0.26
Tl	204.4	0.267	1.787	1.67	1.07	0.28	0.27
Pb	207.2	0.24	1.545	1.61	1.0	0.27	0.25
U	238	0.305	1.54	1.34	0.92	0.23	0.23

*Typical uncertainty ±0.05.

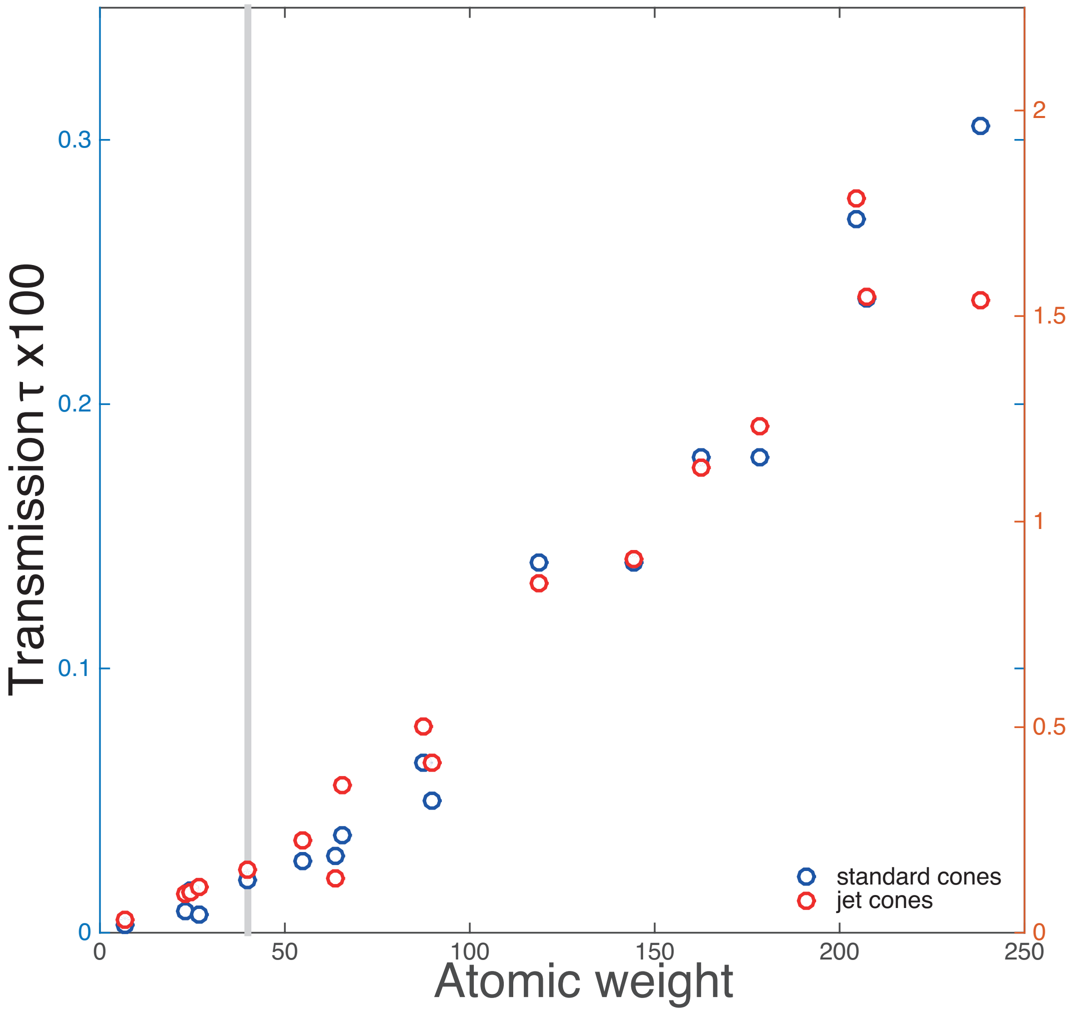

Figure 1: *Transmission as a function of the atomic weight of the elements for the standard (blue) and jet (red) cones. In order to emphasize the similarity between the two arrays, two different scales have been used for transmission.*

Changes in the mass fraction β with transmission are tabulated in Table 3 and shown in Fig. 2. To the points measured with the standard and the jet cones, we added the value β=0 for 100 percent transmission. The plot of β values measured from isotope compositions versus $-\ln\tau$ measured using standard solutions is linear for all the heavy elements, but shows a

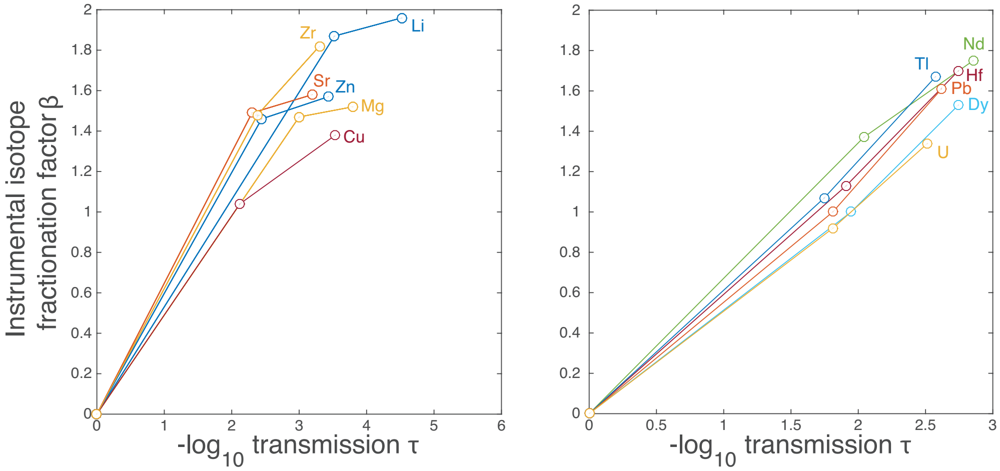

Figure 2: *Instrumental isotope fractionation factor (mass bias)* β *as a function of transmission* τ. *Light elements (left) form a curved array with the point* ($\tau = 1$, $\beta = 0$)*, which can be represented with the function* $\beta = \beta_0 (1 - \tau^{\gamma})$. *Heavier elements (right) with large values of* τ *tend form a linear array with a slope* $\approx \beta_0 \gamma$.

curvature with an inflexion point at $\tau \approx 0.005$ for the lighter elements Li, Mg, Cu, Zn, Sr, and Zr. With jet cones, the ratio $-\beta / \ln \tau$ is remarquably constant ($\approx 0.24 \pm 0.02$) for all elements with the exception of Sn. With standard cones, this ratio is similar, but only for heavy elements. We surmise that part of the scatter is due to incorrect reference isotope compositions. Heavier elements for which τ does not fall below 0.01, do not show an inflexion point. The asymptotic value at low transmission seems to be different for different light elements. It is not known whether this difference should be assigned to incorrect reference isotope compositions adopted for the standards, to different properties of the ion, or to different tuning conditions of the instrument.

A simple approximation accounting for the functional relationship between β and τ is

$$\beta = \beta_0 \left(1 - \tau^{\gamma}\right) \tag{16}$$

where β_0 is the value of β for small transmissions (typically $\beta \approx 2$ for τ <0.002) and γ is a constant to be determined from the measurements. Such a functional relationship has two properties that fit observations: (1) at low transmission, the mass bias β is constant and reproducible, and (2) when τ=1, β=0. This is the case for the lighter elements Li, Mg, Zn, and Sr. For the asymptotic condition $\tau \to 1$

$$\beta \to -\beta_0 \gamma \ln \tau \tag{17}$$

the plot of β vs $-\ln\tau$ then becomes linear with a slope of $\beta_0\gamma$. Fifteen years experience on different MC-ICP-MS operated at low transmission indicates that $1.7 < \beta < 1.9$ [3,4], which suggests a value of $\beta_0 \approx 2$ and therefore $\gamma \approx 0.12$

Since transmission τ increases with atomic weight, the above functional relationship between β and τ explains why external isotope standardization of one element by another element works reasonably well for elements with similar masses, e.g., Cu and Zn [4], Lu and Yb [25], Pb and Tl [26,27], but is somewhat less reliable for elements with masses wide apart, such as Cu and Fe [28] and Rb and Zr [29,30].

5 Conclusions

Increasing MC-ICP-MS transmission reduces instrumental mass fractionation. Transmission of elements above mass 40 increases linearly with the atomic weight, which attests to the effect of thermodynamic reversibility during gas expansion within the interface. Instrumental isotope fractionation obeys an exponential law and at high transmission fractionation can be represented by the relationship $\beta = -0.24 \ln\tau$. The following law

$\beta = \beta_0(1 - \tau^{\gamma})$ represents a good approximation of the process across the range of transmission.

Acknowledgments. Janne Blichert-Toft kindly edited the text. Financial support by Institut National des Sciences de l'Univers (CNRS), Ecole Normale Supérieure de Lyon, Fondation Bullukian, and the Labex Lyon Institute of Origins is gratefully acknowledged. Two anonymous reviewers are thanked for insightful and detailed comments.

References

1. W. A. Russell, D. A. Papanastassiou and T. A. Tombrello, Geochimica et Cosmochimica Acta, 1978, 42, 1075-1090
2. S. R. Hart and A. Zindler, International Journal of Mass Spectrometry and Ion Processes, 1989, 89, 287-301
3. F. Albarede, P. Telouk, J. Blichert-Toft, M. Boyet, A. Agranier and B. Nelson, Geochimica et Cosmochimica Acta, 2004, 68, 2725-2744.
4. C. N. Marechal, P. Telouk and F. Albarede, Chemical Geology, 1999, 156, 251-273.
5. N. Shirai and M. Humayun, Journal of Analytical Atomic Spectrometry, 2011, 26, 1414-1420
6. K. Newman, Journal of Analytical Atomic Spectrometry, 2012, 27, 63-70
7. H. Niu and R. S. I. Houk Spectrochimica Acta Part B: Atomic Spectroscopy, 1996, 51, 779-815.
8. D. Douglas and J. French, Journal of Analytical Atomic Spectrometry, 1988, 3, 743-747.
9. D. M. Chambers and G. M. Hieftje, Spectrochimica Acta Part B: Atomic Spectroscopy, 1991, 46, 761-784.
10. S. D. Tanner, J. Anal. At. Spectrom., 1993, 8, 891-897.
11. P. T. Kirstein, G. S. Kino and W. E. Waters, Space-charge flow, Mc-

Graw Hill, NY, 1967

12. G. R. Brewer, in Focusing of Charged Particles, ed. A. Septier, Academic Press, NY, 1967, vol. II, pp. 23-72.

13. C. C. Cutler and M. Hines, Proceedings of the IRE, 1955, 43, 307-315.

14. S. I. Molokovsky and A. D. Shuskov, Intense Electron and Ion Beams, Springer, Berlin, 2005.

15. M. Reiser, Theory and design of charged particle beams, John Wiley & Sons, Berlin, 2008.

16. N. Kivel, H.-D. Potthast, I. Gnther-Leopold, F. Vanhaecke and D. Günther, Journal of Analytical Atomic Spectrometry, 2015.

17. G. R. Gillson, D. J. Douglas, J. E. Fulford, K. W. Halligan and S. D. Tanner, Analytical Chemistry, 1988, 60, 1472-1474.

18. S. D. Tanner, Spectrochimica Acta Part B: Atomic Spectroscopy, 1992, 47, 809-823.

19. F. Vanhaecke, R. Dams and C. Vandecasteele, Journal of Analytical Atomic Spectrometry, 1993, 8, 433-438.

20. K. G. Heumann, S. M. Gallus, G. Rdlinger and J. Vogl, Journal of Analytical Atomic Spectrometry, 1998, 13, 1001-1008.

21. L. Yang, C. Peter, U. Panne and R. E. Sturgeon, Journal of Analytical Atomic Spectrometry, 2008, 23, 1269-1274.

22. G. H. Fontaine, B. Hattendorf, B. Bourdon and D. Gnther, Journal of Analytical Atomic Spectrometry, 2009, 24, 637-648.

23. D. Malinovsky, A. Stenberg, I. Rodushkin, H. Andren, J. Ingri, B. hlander and D. C. Baxter, Journal of Analytical Atomic Spectrometry, 2003, 18, 687-695.

24. R. Santos, M. J. Canto Machado, I. Ruiz, K. Sato and M. T. S. D. Vasconcelos, Journal of Analytical Atomic Spectrometry, 2007, 22, 783-790

25. J. Blichert-Toft, C. Chauvel and F. Albarede, Contributions to Mineralogy and Petrolgy, 1997, 127, 248-260.

26. M. Rehkämper and A. N. Halliday, International Journal of Mass Spectrometry, 1998, 181, 123-133.

27. W. M. White, F. Albarede and P. Telouk, Chemical Geology, 2000, 167, 257-270.

28. K. Kehm, E. H. Hauri, C. M. O. D. Alexander and R. W. Carlson, Geochimica et Cosmochimica Acta, 2003, 67, 2879-2891.

29. O. Nebel, K. Mezger, E. E. Scherer and C. Münker, International Journal of Mass Spectrometry, 2005, 246, 10-18.

30. L. Yang, C. Peter, U. Panne and R. E. Sturgeon, Journal of Analytical Atomic Spectrometry, 2008, 23, 1269-1274.

31. L. Chan, J. Edmond, G. Thompson and K. Gillis, Earth and Planetary Science Letters, 1992, 108, 151-160.

32. E. J. Catanzaro, T. J. Murphy, E. L. Garner and W. R. Shields, Journal of Research National Bureau of Standards A, 1966, 70, 453-458.

33. I. Raczek, K. P. Jochum and A. W. Hofmann, Geostandards Newsletter, 2003, 27, 173-179.

34. M. Nomura, K. Kogure and M. Okamoto, International Journal of Mass Spectrometry and Ion Physics, 1983, 50, 219-227.

35. N. McNaughton and K. Rosman, Geochimica et Cosmochimica Acta, 1991, 55, 499-504.

36. G. J. Wasserburg, S. B. Jacobsen, D. J. DePaolo, M. T. McCulloch and T. Wen, Geochimica et Cosmochimica Acta, 1981, 45, 2311-2323.

37. T.-L. Chang, W.-J. Li, M.-T. Zhao, J. Wang and Q.-Y. Qian, International Journal of Mass Spectrometry, 2001, 207, 13-17.

38. L. Dunstan, J. Gramlich, I. Barnes and W. Purdy, Journal of Research of the National Bureau of Standards, 1980, 85, 1-10.

39. J. Eisele, W. Abouchami, S. J. G. Galer and A. W. Hofmann, Geochemistry, Geophysics, Geosystems, 2003, 4, doi: 10.1029/2002GC000339.

40. J. Hiess, D. J. Condon, N. McLean and S. R. Noble, Science, 2012, 335,

1610-1614.